Original Article | Technology, Experiment, and Physics

eISSN 2005-8330
https://doi.org/10.3348/kjr.2020.0716
Korean J Radiol 2021;22(7):1194-1202

Korean Journal of Radiology
KJR

Arterial Spin Labeling Magnetic Resonance Imaging in Healthy Adults: Mathematical Model Fitting to Assess Age-Related Perfusion Pattern

Ying Hu, Rongbo Liu, Fabao Gao

All authors: Department of Radiology, West China Hospital, Sichuan University, Chengdu, China

Objective: To investigate the age-dependent changes in regional cerebral blood flow (CBF) in healthy adults by fitting mathematical models to imaging data.

Materials and Methods: In this prospective study, 90 healthy adults underwent pseudo-continuous arterial spin labeling imaging of the brain. Regional CBF values were extracted from the arterial spin labeling images of each subject. Multivariable regression with the Akaike information criterion, link test, and F test (Ramsey's regression equation specification error test) was performed for 7 models in every brain region to determine the best mathematical model for fitting the relationship between CBF and age.

Results: Of all 87 brain regions, 68 brain regions were best fitted by cubic models, 9 brain regions were best fitted by quadratic models, and 10 brain regions were best fitted by linear models. In most brain regions (global gray matter and the other 65 brain regions), CBF decreased nonlinearly with aging, and the rate of CBF reduction decreased with aging, gradually approaching 0 after approximately 60. CBF in some regions of the frontal, parietal, and occipital lobes increased nonlinearly with aging before age 30, approximately, and decreased nonlinearly with aging for the rest of life.

Conclusion: In adults, the age-related perfusion patterns in most brain regions were best fitted by the cubic models, and age-dependent CBF changes were nonlinear.

Keywords: *Arterial spin labeling; Magnetic resonance imaging; Cerebral blood flow; Aging; Mathematical model fitting*

INTRODUCTION

Cerebral blood flow (CBF) refers to the delivery rate of arterial blood to the capillary bed in the brain tissue, and it characterizes cerebral perfusion quantitatively [1,2]. CBF is a critical biomarker of cerebral metabolism and functional activity [3]. Various techniques have been developed to measure CBF, including positron emission tomography (PET), single-photon emission computed tomography (SPECT), dynamic contrast-enhanced magnetic resonance imaging (MRI), dynamic susceptibility contrast MRI, and arterial spin labeling (ASL). ASL perfusion imaging, a noninvasive MRI method that does not require the use of exogenous tracer and ionizing radiation, has been reported to allow the direct quantification of the absolute CBF using arterial blood water as an endogenous tracer [1,2,4-6].

Aging is an important risk factor for cerebrovascular and neurodegenerative diseases [7,8]. CBF is a marker of brain activity, which could play a central role in unveiling the biological processes involved in aging [3]. To properly interpret CBF changes in these disease conditions, it is essential to understand normal age-related CBF changes [2,9]. Previous studies have reported the age-related CBF reduction in the entire brain or some brain regions [10-13] using PET and SPECT, especially a continuous age-related decrease during adulthood. Kety [14] reviewed the studies

Received: April 8, 2020 **Revised:** January 1, 2021
Accepted: January 8, 2021
Corresponding author: Fabao Gao, MD, PhD, Department of Radiology, West China Hospital, Sichuan University, No. 37 Guoxue Alley, Wuhou District, Chengdu, Sichuan 610041, China.
• E-mail: gaofabao@yahoo.com

Korean Journal of Radiology
KJR

on CBF obtained through the nitrous oxide technique and found a rapid reduction in CBF from childhood to adolescence, followed by a more gradual but progressive decline throughout adult life [14]. Recently, several studies have investigated the age-related CBF changes using various ASL techniques, including continuous ASL (CASL), pulsed ASL (PASL), and pseudo-continuous ASL (pCASL) [1-3,15]. These studies have shown a significant decline across most parts of the brain. Notably, a relatively higher regional CBF has also been detected in older adults than in younger subjects [2,3].

To date, most of the studies on age-related CBF changes directly divided the subjects into different age groups to compare the differences [16-18] or performed linear regression to analyze the correlation between age and CBF [2,15,19]. Nonlinear trajectories of CBF changes have recently been reported during brain maturation in infants and young children using pCASL [20]. Aging processes in adults may also follow certain patterns or trajectories. However, to our knowledge, no studies have evaluated the trajectory of CBF changes during aging in adults.

In the present study, we measured the regional CBF values in a relatively large sample of healthy adults using pCASL and assessed the age-related perfusion pattern by determining the trajectory of age-dependent CBF changes in each brain region by systematically fitting mathematical models to the CBF data.

MATERIALS AND METHODS

Participants

The Institutional Review Board of our hospital approved this prospective study. All subjects provided written informed consent before the MRI examination. We performed the Mini-Mental State Examination (MMSE) and Mattis Dementia Rating Scale (MDRS) to select cognitively normal participants (MMSE scores > 24 or MDRS scores > 130). One hundred and three subjects with normal cognition, who had no history of brain tumor, trauma, brain injury, cerebrovascular disorder, carotid stents or dentures, neurologic or cardiac disease, hypertension, diabetes, renal disease, alcoholism, or metal implants in the body, were selected for this study. One subject was excluded because of claustrophobia. After the MRI examination, two experienced neuro-radiologists visually inspected the conventional MRI and magnetic resonance angiography (MRA) findings for any intracranial (3 subjects) or vascular (9 subjects) lesions. A total of 90 right-handed healthy adults (mean age, 49.47 years; age range, 20–77 years; women, 47; men, 43) were enrolled. The age distributions of the subjects are listed in Table 1. All subjects refrained from alcohol, caffeine, nicotine, and vigorous exercise 24 hours before MRI examination.

MRI Technique

All images were obtained using a 3T MRI scanner (Signa HDxt, General Electric) with an 8-channel head coil. Phase-contrast MRA was performed to identify the cerebrovascular disease. Conventional images, including axial T2-weighted, axial fluid-attenuated inversion-recovery, and axial three-dimensional T1-weighted images, were acquired and used to exclude subjects with intracranial lesions. The whole-brain perfusion data were obtained using a pCASL sequence, with a three-dimensional background-suppressed fast-spin-echo acquisition and the following parameters: repetition time (TR), 4912 ms; echo time (TE), 9.8 ms; number of signals acquired, 3; field of view (FOV), 24 x 24 cm^2; reconstructed matrix, 64 x 64; section thickness, 4 mm; number of sections, 30; sampling points on 8 spirals, 512; labeling duration, 1525 ms; post-labeling delays (PLDs), 2025 ms; control/label pairs, 30; acquisition time, 4 minutes 52 seconds.

Analysis of MRI Data

All imaging data analyses were completed using MATLAB R2014a (MathWorks), statistical parametric mapping (SPM8) (http://www.fil.ion.ucl.ac.uk/spm/software/spm8/), ADW4.5 (GE workstation), and WFU Pickatlas (http://fmri.wfubmc.edu/software/PickAtlas).

The raw data of the ASL images were imported to a GE workstation (ADW4.5) to generate CBF maps. The CBF maps underwent preprocessing, including motion correction, registration, partial volume correction, normalization, and smoothing. The registration of the CBF images was

Table 1. The Age Distribution of the Subjects

Age Range (Years)	N	Proportion (%, N/Total)	Mean (Years)
20–30	17	18.89	23.8
31–40	16	17.78	35.8
41–50	17	18.89	46.6
51–60	19	21.11	55.7
61–77	21	23.33	66.8
Total (20–77)	90	100	49.5

N = number

https://doi.org/10.3348/kjr.2020.0716

performed using the segmentation transformation matrix generated from the T1-weighted images and spatially normalized to the Montreal Neurological Institute template. Smoothing was performed using an isotropic kernel of 6 mm. Subsequently, 87 masks of the volume of interest (VOI) (global gray matter and other 86 VOIs) were generated in WFU Pickatlas (Supplementary Fig. 1). The frontal lobe, parietal lobe, temporal lobe, occipital lobe, limbic system, and deep gray matter were divided into 28, 12, 14, 12, 12, and 8 VOIs, respectively (Supplementary Table 1). Finally, the CBF values of the 87 VOIs were extracted from the preprocessed CBF maps using the corresponding masks. In this study, the brain region is equivalent to the VOI.

Statistical Analysis

The statistical analysis was performed using Stata (version 15.0; Stata Corp.). Multivariable regression was performed to determine the mathematical best-fitting model to describe the relationship between CBF and age. Seven forms of models can be obtained according to the number and combination of selecting age variables (age, age^2, age^3). Thus, 7 regression models (4 cubic models, 2 quadratic models, and 1 linear model) were fitted to the data using Stata. Gender was used as the control variable. Our study tested the effect of the interaction between age and gender and showed that the interaction of gender and age had no significant effect on CBF. The mathematical formulas for the 7 models are as follows:

Model 1: $CBF = \beta_1 age + \beta_2 gender + constant$;
Model 2: $CBF = \beta_1 age^2 + \beta_2 gender + constant$;
Model 3: $CBF = \beta_1 age^3 + \beta_2 gender + constant$;
Model 4: $CBF = \beta_1 age + \beta_2 age^2 + \beta_3 gender + constant$;
Model 5: $CBF = \beta_1 age + \beta_2 age^3 + \beta_3 gender + constant$;
Model 6: $CBF = \beta_1 age^2 + \beta_2 age^3 + \beta_3 gender + constant$;
Model 7: $CBF = \beta_1 age + \beta_2 age^2 + \beta_3 age^3 + \beta_4 gender + constant$;

where β (n) is the regression coefficient. The value of gender was 0 for women and 1 for men.

We compared the models using the Akaike information criterion (AIC) [21,22], the link test [23,24], and the F test to select the best-fitted model. In this study, the F test used Ramsey's regression equation specification error test [25,26]. The link and F tests were used to check whether the model's function form was correct. The link and F test outcomes with *p* values greater than 0.05 indicate no problem with the model's function form. The AIC is a method for model selection that compares the models' effectiveness while penalizing their complexities [21,22]. The AIC has the advantage of minimizing the potential overfitting caused by incorporating too many parameters into the models (the smaller the AIC value, the better the model). Therefore, the model with the smallest AIC value among those with *p* values greater than 0.05 in the link and F tests was selected as the best regression model. The flowchart for the statistical analysis is shown in Figure 1.

RESULTS

The Best-Fitting Model of Each VOI

The CBF value for each VOI is expressed as the mean ± standard deviation in Supplementary Table 1. The values of AIC and the results of the link and F tests for the 7 models for each VOI are listed in Supplementary Table 2. Most of the 87 VOIs (68) were best fitted by the cubic models (model 5, 8 VOIs; model 6, 50 VOIs; model 7, 10 VOIs), 9 were best fitted by the quadratic models (model 2, 1 VOI; model 4, 8 VOIs), and 10 were best fitted by the linear model (model 1, 10 VOIs). No VOI was fitted by model 3. The best-fitting models for all the brain regions are presented in Table 2.

The Age-Related Changes in Regional CBF by Model

The equations of the best-fit model for each VOI are listed in Supplementary Table 3. The derivative function of each equation is listed in Supplementary Table 3. A function is increasing if it has a derivative value of more than 0 and decreasing if the derivative value is less than 0. Moreover, the absolute value of the derivative reflects the speed of the functional changes.

The VOIs Best-Fitted by Model 1 (Linear Model)

In our study, some VOIs in the occipital lobe (6 VOIs), parietal lobe (3 VOIs), and temporal lobe (1 VOI) were best fitted by model 1. We found that the derivatives of the functions in these VOIs were constant and less than 0. Therefore, CBF values in these brain regions decreased linearly with age.

The VOIs Best Fitted by Model 2 (Quadratic Model)

One VOI in the occipital lobe was best fitted by model 2. The derivative of the function for this VOI was less than 0, and the derivative's absolute value increased with age. Therefore, the CBF value in this brain region decreased

https://doi.org/10.3348/kjr.2020.0716

Korean Journal of Radiology
KJR

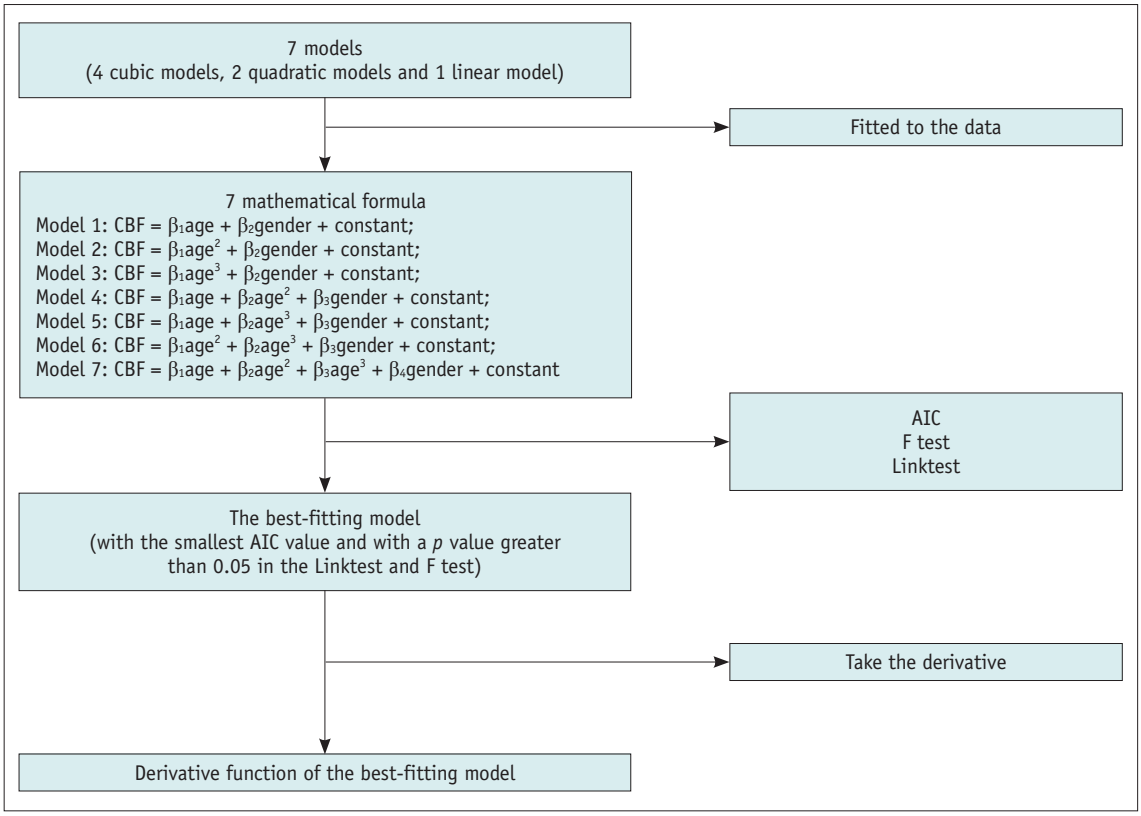

Fig. 1. Flowchart of the analytical methods. AIC = Akaike information criterion

nonlinearly with age, and the rate of CBF reduction increased with age.

The VOIs Best Fitted by Model 4 (Quadratic Model), Model 5 (Cubic Model), and Model 6 (Cubic Model)

Eight VOIs in the deep gray matter (6 VOIs) and the parietal (1 VOI) and frontal (1 VOI) lobes were best fitted by model 4. Eight VOIs in the frontal lobe (4 VOIs), parietal lobe (1 VOI), temporal lobe (1 VOI), limbic system (1 VOI), and the deep gray matter (1 VOI) were best fitted by model 5. Forty-nine VOIs in the frontal lobe (20 VOIs), temporal lobe (12 VOIs), limbic system (11 VOIs), occipital lobe (3 VOIs), parietal lobe (2 VOIs), and deep gray matter (1 VOI) were best fitted by model 6. In addition, the global gray matter was best fitted by model 6.

The values of the derivatives of the functions in the VOIs that were best fitted by model 4 (quadratic model), model 5 (cubic model), and model 6 (cubic model) were less than 0 before the age of approximately 60 years, and the derivatives' absolute values in these VOIs decreased with age. Thus, the CBF for the VOIs best fitted by models 4, 5, and 6 decreased with age nonlinearly. For these VOIs, the rate of CBF reduction decreased with aging and gradually approached 0 after approximately 60 years.

The VOIs Best Fitted by Model 7 (Cubic Model)

Finally, some VOIs in the frontal lobe (3 VOIs), parietal lobe (5 VOIs), and occipital lobe (2 VOIs) were best fitted by model 7. For these VOIs, the CBF increased nonlinearly with aging before approximately 30 years for the derivatives of the functions in these VOIs were more than 0 before the age of approximately 30 years; the CBF decreased nonlinearly with aging for the rest of adult life for the derivatives of the functions in these VOIs were less than 0 after approximately 30 years. Figure 2 shows the fitted lines of the best model for 6 typical brain regions.

DISCUSSION

Our results demonstrated that most brain regions (68 VOIs) were best fitted by cubic models. CBF in most brain regions decreased nonlinearly with aging in adults, and the rate of CBF reduction decreased with aging and gradually approached 0 after approximately 60 years. We also found that the CBF in some brain regions increased nonlinearly with aging before approximately 30 years and decreased

 https://doi.org/10.3348/kjr.2020.0716

Table 2. The Best-Fitting Model of Each VOI

Lobes (VOI)	Linea Model*	Quadratic Model*		Cubic Model*		
	Model 1	Model 2	Model 4	Model 5	Model 6	Model 7
Frontal Lobe (28)	-	-	1 (Frontal_Inf_Oper_R)	4 (Frontal_Inf_Orb_L,Frontal_Inf_Tri_L,Frontal_Mid_Orb_L,Insula_R)	20 (Frontal_Inf_Oper_L,Frontal_Inf_Orb_R,Frontal_Inf_Tri_R,Frontal_Med_Orb_L,Frontal_Med_Orb_R,Frontal_Mid_L,Frontal_Mid_R, Frontal_Mid_Orb_R,Frontal_Sup_L,Frontal_Sup_R,Frontal_Sup_Medial_L,Frontal_Sup_Medial_R,Frontal_Sup_Orb_L,Frontal_Sup_Orb_R,Insula_L,Precentral_L,Precentral_R, Rectus_L,Rolandic_Oper_L,Rolandic_Oper_R)	3 (Paracentral_Lobule_L,Paracentral_Lobule_R,Rectus_R)
Parietal Lobe (12)	3 (Angular_L,Angular_R,Parietal_Inf_L)	-	1 (SupraMarginal_R)	1 (SupraMarginal_L)	2 (Parietal_Inf_R,Precuneus_R)	5 (Parietal_Sup_L,Parietal_Sup_R,Postcentral_L,Postcentral_R,Precuneus_L)
Temporal Lobe (14)	1 (Fusiform_R)	-	-	1 (Heschl_R)	12 (Fusiform_L,Heschl_L,Temporal_Inf_L,Temporal_Inf_R,Temporal_Mid_L,Temporal_Mid_R,Temporal_Pole_Mid_L,Temporal_Pole_Mid_R,Temporal_Pole_Sup_L,Temporal_Pole_Sup_R,Temporal_Sup_L,Temporal_Sup_R)	-
Occipital Lobe (12)	6 (Calcarine_L,Cuneus_R,Occipital_Inf_L,Occipital_Inf_R,Occipital_Mid_L,Occipital_Mid_R)	1 (Occipital_Sup_R)	-	-	3 (Calcarine_R,Lingual_L,Lingual_R)	2 (Cuneus_L,Occipital_Sup_L)
Limbic System (12)	-	-	-	1 (Amygdala_R)	11 (Amygdala_L,Cingulum_Ant_L,Cingulum_Ant_R,Cingulum_Mid_L,Cingulum_Mid_R,Cingulum_Post_L,Cingulum_Post_R,Hippocampus_L,Hippocampus_R,ParaHippocampal_L,ParaHippocampal_R)	-
Deep GM (8)	-	-	6 (Caudate_L,Caudate_R,Pallidum_L,Pallidum_R,Putamen_L,Putamen_R)	1 (Thalamus_L)	1 (Thalamus_R)	-
Global GM (1)	-	-	-	-	1 (Global GM)	-
Total (87)	10	1	8	8	50	10

Model 1: CBF = $\beta_1$age + $\beta_2$gender + constant; Model 2: CBF = $\beta_1$age^2 + $\beta_2$gender + constant; Model 4: CBF = $\beta_1$age + $\beta_2$age^2 + $\beta_3$gender + constant; Model 5: CBF = $\beta_1$age + $\beta_2$age^3 + $\beta_3$gender + constant; Model 6: CBF = $\beta_1$age^2 + $\beta_2$age^3 + $\beta_3$gender + constant; Model 7: CBF = $\beta_1$age + $\beta_2$age^2 + $\beta_3$age^3 + $\beta_1$gender + constant. *Data are the numbers of VOIs. Ant = anterior, CBF = cerebral blood flow, GM = gray matter, Inf = inferior, Mid = medial, Oper = operculum, Orb = orbit, Sup = superior, Tri = triangle, VOI = volume of interest

Korean Journal of Radiology
KJR

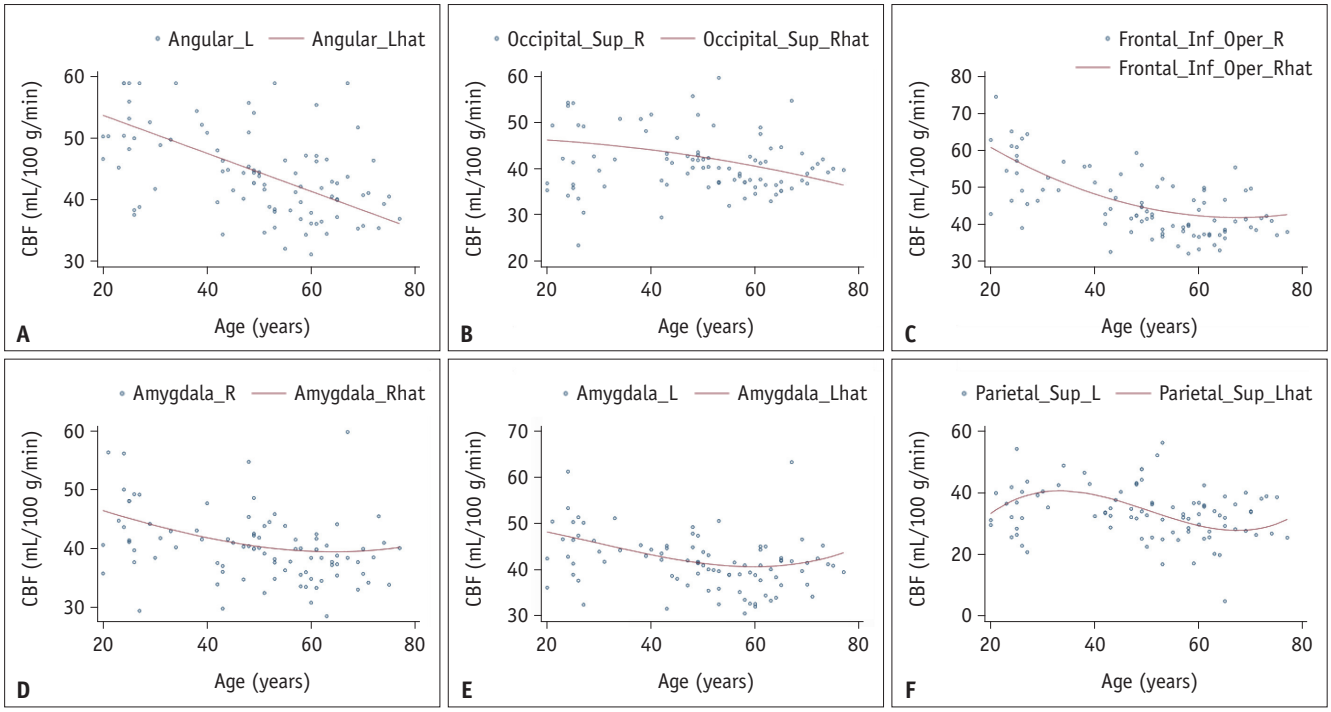

Fig. 2. The fitted lines of 6 typical brain regions. In each subplot, the variable on the horizontal axis is age. the variable on the vertical axis is CBF, the small circles represent the true CBF value of each observation, and the red line is the fitting line of the best model. **A.** The best-fitting model for the left lateral Angular is model 1 (CBF = -0.2233695age + 55.56486). **B.** The best-fitting model for the right lateral Occipital_Sup is model 2 (CBF = -0.0006218age^2 + 43.67833). **C.** The best-fitting model for the right lateral Frontal_Inf_Oper is model 4 (CBF = 0.0084219age^2 - 1.135935age + 80.03286). **D.** The best-fitting model for the right lateral amygdala is model 5 (CBF = 0.0000237age^3 - 0.2954774age + 52.20578). **E.** The best-fitting model for the left lateral amygdala is model 6 (CBF = 0.0000951age^3 - 0.0085284age^2 + 50.8373). **F.** The best-fitting model for the left lateral Parietal_Sup is model 7 (CBF = 0.0006103age^3 - 0.0923499age^2 + 4.223066age-22.11918). CBF = cerebral blood flow

nonlinearly with aging for the rest of life.

Studies that compared ASL and PET have demonstrated the utility of ASL for accurate and reproducible CBF measurements [27]. In the present study, the CBF values for the entire GM and the regional brain regions were consistent with those obtained in previous studies [28-30]. The mean CBF for the entire GM in our study was 40.76 mL/100 g/min. Previous ASL studies reported the average CBF for the entire GM ranging from 39.3 mL/100 g/min to 52.1 mL/100 g/min [30].

Age-related CBF decrease in the entire GM or regions of the brain has been observed in several previous studies using various imaging modalities [11,15,31,32]. Our results are in general agreement with those of previous reports. However, our study further demonstrated a nonlinear correlation between CBF and age rather than the linear age-related perfusion pattern most previous studies have shown [11,18,31,32]. This contradiction may be due to the different statistical analyses. Previous studies directly performed a linear regression or Pearson correlation analysis. We performed a multivariable regression analysis to explore the age-related perfusion pattern. In our study, both linear and nonlinear models were used to fit the relationship between CBF and age. Heo proposed that a quadratic function may better capture the relationship between age and CBF instead of a strictly linear function [33]. Our results generally agree with the findings of Kety [14]. Kety [14] found a rapid decrease in CBF around puberty, which continued until the third decade, followed by a more gradual but progressive reduction throughout the remaining age span. They favored a rapid, followed by a more gradual, fall with advancing years, which means that the CBF decreased nonlinearly with age in adults. Previous studies have indicated that an age-related CBF decrease is mainly or exclusively a consequence of reduced metabolic needs. The diminished metabolic demands of the brain could be the result of a simple loss of neurons, a progressive deterioration in certain essential cellular components, a decrease in neuronal interconnections and interaction, or a reduced functional demand as a result of the psychological and social changes that occur during the aging process or other fundamental causes [14,34-36]. Therefore, age-related perfusion patterns may reflect the pattern of physiological

 https://doi.org/10.3348/kjr.2020.0716

and structural changes in the brain during aging.

In our study, we found that the CBF in some regions of the frontal, parietal, and occipital lobes, which were best fitted by model 7, increased nonlinearly with aging before approximately 30 years and decreased nonlinearly with aging for the rest of life. Previous studies have also found an age-related increase in CBF in some brain regions [2,3,37]. These brain regions are mainly distributed in the bilateral white matter regions of the frontal and parietal lobes [37] and some regions of the temporal lobe, occipital lobe, and deep gray matter [2,3]. In previous studies, the brain regions that had an age-related CBF increase showed a continuous age-related increase when they used linear regression analysis [3,37], or it was not clear whether there was a continuous age-related increase because they used group comparison to determine the CBF differences between the older and younger groups [2]. In our study, the brain regions that had an age-related CBF increase showed nonlinear increments in perfusion patterns before approximately 30 years, followed by nonlinear decrements with aging for the rest of life. We hypothesized that the different age-related increasing patterns were due to different statistical analysis methods. The physiological mechanism underlying this increasing pattern was not clear. Previous studies speculated that the regional increase in CBF may be attributed to a compensatory response to aging [2], such as an increase in compensatory neural activity during aging [3]. Brain regions with an age-related CBF increase are relatively preserved compared with other regions during normal aging [2,3]. Moreover, our results also found that the age-related increasing pattern in the frontal, parietal, and occipital lobes did not last for the entire adult period. These regions also showed an age-related decrease after approximately 30 years. This may indicate that the compensatory response of CBF to aging described previously gradually loses its effect after 30 years.

This study has several limitations. We used the same PLD for all subjects. However, arterial transit time may differ between young and older subjects because of blood velocity differences in the arteries. Although single-PLD was recommended as a clinical standard scanning protocol [38] and the PLD used in the present study was recommended by consensus [38], multi-PLD can provide a more accurate CBF assessment. Another limitation is that our study was cross-sectional. Although our sample size was relatively large, a cohort study would be more appropriate to investigate the longitudinal age-related CBF change in each subject to reduce inter-subject variation.

In conclusion, we investigated the trajectory of age-dependent CBF changes in different brain regions in adults by systematically fitting mathematical models to CBF data using multivariable regression. Compared with the quadratic and linear models, the cubic model was the best-fitting model for global gray matter and most brain regions. We demonstrated the age-related perfusion pattern in each brain region by analyzing the formulas of the best-fitted model. In the global gray matter and most brain regions, CBF decreases nonlinearly with aging. CBF in some regions of the frontal, parietal, and occipital lobes increased nonlinearly with aging before approximately 30 years and decreased nonlinearly with aging for the rest of life.

Supplement

The Supplement is available with this article at https://doi.org/10.3348/kjr.2020.0716.

Conflicts of Interest

The authors have no potential conflicts of interest to disclose.

Acknowledgments

We would like to acknowledge the work of our doctoral students in our department who worked many days and nights performing MR imaging scanning on the volunteers. We would also like to thank the volunteers who traveled long distances to our hospital and actively cooperate with our MR scanning.

Author Contributions

Conceptualization: all authors. Data curation: all authors. Formal analysis: all authors. Funding acquisition: Fabao Gao. Investigation: all authors. Methodology: all authors. Project administration: Ying Hu, Fabao Gao. Resources: all authors. Software: all authors. Supervision: all authors. Validation: all authors. Visualization: all authors. Writing—original draft: Ying Hu. Writing—review & editing: Ying Hu, Fabao Gao.

ORCID iDs

Ying Hu
https://orcid.org/0000-0002-0943-2382
Rongbo Liu
https://orcid.org/0000-0003-0135-7514

Fabao Gao
https://orcid.org/0000-0003-2257-3275

REFERENCES

1. Biagi L, Abbruzzese A, Bianchi MC, Alsop DC, Del Guerra A, Tosetti M. Age dependence of cerebral perfusion assessed by magnetic resonance continuous arterial spin labeling. *J Magn Reson Imaging* 2007;25:696-702
2. Zhang N, Gordon ML, Ma Y, Chi B, Gomar JJ, Peng S, et al. The age-related perfusion pattern measured with arterial spin labeling MRI in healthy subjects. *Front Aging Neurosci* 2018;10:214
3. Preibisch C, Sorg C, Förschler A, Grimmer T, Sax I, Wohlschläger AM, et al. Age-related cerebral perfusion changes in the parietal and temporal lobes measured by pulsed arterial spin labeling. *J Magn Reson Imaging* 2011;34:1295-1302
4. Campbell AM, Beaulieu C. Pulsed arterial spin labeling parameter optimization for an elderly population. *J Magn Reson Imaging* 2006;23:398-403
5. Wintermark M, Sesay M, Barbier E, Borbély K, Dillon WP, Eastwood JD, et al. Comparative overview of brain perfusion imaging techniques. *Stroke* 2005;36:e83-e99
6. Wang J, Licht DJ, Jahng GH, Liu CS, Rubin JT, Haselgrove J, et al. Pediatric perfusion imaging using pulsed arterial spin labeling. *J Magn Reson Imaging* 2003;18:404-413
7. Elias MF, D'Agostino RB, Elias PK, Wolf PA. Neuropsychological test performance, cognitive functioning, blood pressure, and age: the Framingham Heart Study. *Exp Aging Res* 1995;21:369-391
8. Farmer ME, Kittner SJ, Abbott RD, Wolz MM, Wolf PA, White LR. Longitudinally measured blood pressure, antihypertensive medication use, and cognitive performance: the Framingham Study. *J Clin Epidemiol* 1990;43:475-480
9. Zhang N, Gordon ML, Goldberg TE. Cerebral blood flow measured by arterial spin labeling MRI at resting state in normal aging and Alzheimer's disease. *Neurosci Biobehav Rev* 2017;72:168-175
10. Pantano P, Baron JC, Lebrun-Grandié P, Duquesnoy N, Bousser MG, Comar D. Regional cerebral blood flow and oxygen consumption in human aging. *Stroke* 1984;15:635-641
11. Martin AJ, Friston KJ, Colebatch JG, Frackowiak RS. Decreases in regional cerebral blood flow with normal aging. *J Cereb Blood Flow Metab* 1991;11:684-689
12. Pagani M, Salmaso D, Jonsson C, Hatherly R, Jacobsson H, Larsson SA, et al. Regional cerebral blood flow as assessed by principal component analysis and ^{99m}Tc-HMPAO SPET in healthy subjects at rest: normal distribution and effect of age and gender. *Eur J Nucl Med Mol Imaging* 2014;29:67-75
13. Devous MD Sr, Stokely EM, Chehabi HH, Bonte FJ. Normal distribution of regional cerebral blood flow measured by dynamic single-photon emission tomography. *J Cereb Blood Flow Metab* 1986;6:95-104
14. Kety SS. Human cerebral blood flow and oxygen consumption as related to aging. *J Chronic Dis* 1956;3:478-486
15. Parkes LM, Rashid W, Chard DT, Tofts PS. Normal cerebral perfusion measurements using arterial spin labeling: reproducibility, stability, and age and gender effects. *Magn Reson Med* 2004;51:736-743
16. Chen JJ, Rosas HD, Salat DH. Age-associated reductions in cerebral blood flow are independent from regional atrophy. *Neuroimage* 2011;55:468-478
17. Liu W, Lou X, Ma L. Use of 3D pseudo-continuous arterial spin labeling to characterize sex and age differences in cerebral blood flow. *Neuroradiology* 2016;58:943-948
18. Hasan KM, Ali H, Shad MU. Atlas-based and DTI-guided quantification of human brain cerebral blood flow: feasibility, quality assurance, spatial heterogeneity and age effects. *Magn Reson Imaging* 2013;31:1445-1452
19. Hurvich CM, Tsai CL. Bias of the corrected AIC criterion for underfitted regression and time series models. *Biometrika* 1991;78:499-509
20. Wong AM, Liu HL, Tsai ML, Schwartz ES, Yeh CH, Wang HS, et al. Arterial spin-labeling magnetic resonance imaging of brain maturation in early childhood: mathematical model fitting to assess age-dependent change of cerebral blood flow. *Magn Reson Imaging* 2019;59:114-120
21. Cavanaugh JE. Unifying the derivations for the Akaike and corrected Akaike information criteria. *Stat Probab Lett* 1997;33:201-208
22. Akaike H. A new look at the statistical model identification. *IEEE T Automat Contr* 1974;19:716-723
23. Tukey JW. One degree of freedom for non-additivity. *Biometrics* 1949;5:232-242
24. Pregibon D. Goodness of link tests for generalized linear models. *J R Stat Soc: Series C (Applied Statistics)* 1980;29:15-24
25. Ramsey JB. Tests for specification errors in classical linear least-squares regression analysis. *J R Stat Soc: Series B (Methodological)* 1969;31:350-371
26. Ramsey JB, Zarembka P. Specification error tests and alternative functional forms of the aggregate production function. *J Am Stat Assoc* 1971;66:471-477
27. Fan AP, Jahanian H, Holdsworth SJ, Zaharchuk G. Comparison of cerebral blood flow measurement with [^{15}O]-water positron emission tomography and arterial spin labeling magnetic resonance imaging: a systematic review. *J Cereb Blood Flow Metab* 2016;36:842-861
28. Leenders KL, Perani D, Lammertsma AA, Heather JD, Buckingham P, Healy MJ, et al. Cerebral blood flow, blood volume and oxygen utilization. Normal values and effect of age. *Brain* 1990;113:27-47
29. Yamaguchi T, Kanno I, Uemura K, Shishido F, Inugami A, Ogawa T, et al. Reduction in regional cerebral metabolic rate of oxygen during human aging. *Stroke* 1986;17:1220-1228
30. Petersen ET, Mouridsen K, Golay X. The QUASAR reproducibility

study, part II: results from a multi-center Arterial Spin Labeling test-retest study. *Neuroimage* 2010;49:104-113
31. Liu Y, Zhu X, Feinberg D, Guenther M, Gregori J, Weiner MW, et al. Arterial spin labeling MRI study of age and gender effects on brain perfusion hemodynamics. *Magn Reson Med* 2012;68:912-922
32. Buijs PC, Krabbe-Hartkamp MJ, Bakker CJ, de Lange EE, Ramos LM, Breteler MM, et al. Effect of age on cerebral blood flow: measurement with ungated two-dimensional phase-contrast MR angiography in 250 adults. *Radiology* 1998;209:667-674
33. Heo S, Prakash RS, Voss MW, Erickson KI, Ouyang C, Sutton BP, et al. Resting hippocampal blood flow, spatial memory and aging. *Brain Res* 2010;1315:119-127
34. Shefer VF. Absolute number of neurons and thickness of the cerebral cortex during aging, senile and vascular dementia, and Pick's and Alzheimer's diseases. *Neurosci Behav Physiol* 1973;6:319-324
35. Henderson G, Tomlinson BE, Gibson PH. Cell counts in human cerebral cortex in normal adults throughout life using an image analysing computer. *J Neurol Sci* 1980;46:113-136
36. Brody H. Organization of the cerebral cortex. III. A study of aging in the human cerebral cortex. *J Comp Neurol* 1955;102:511-516
37. Lu H, Xu F, Rodrigue KM, Kennedy KM, Cheng Y, Flicker B, et al. Alterations in cerebral metabolic rate and blood supply across the adult lifespan. *Cereb Cortex* 2010;21:1426-1434
38. Alsop DC, Detre JA, Golay X, Günther M, Hendrikse J, Hernandez-Garcia L, et al. Recommended implementation of arterial spin-labeled perfusion MRI for clinical applications: a consensus of the ISMRM perfusion study group and the European consortium for ASL in dementia. *Magn Reson Med* 2015;73:102-116

https://doi.org/10.3348/kjr.2020.0716